Journal of Advanced Zoology
ISSN: 0253-7214
Volume 44 Issue S-6 Year 2023 Page 2402:2417

Spatio-Temporal Evaluation of Temperature-Based ET_0 Estimation Methods in Northwestern Iran

Simin Ganjei[a*], Jalal Shiri[a], Sepideh Karimi[b]

[a*] *Department of Water Engineering, Faculty of Agriculture, University of Tabriz, Tabriz, Iran.*
siminganjei@yahoo.com; j_shiri2005@yahoo.com
[b] *Water Engineering and Science Research Institute, University of Tabriz, Tabriz, Iran.*
Karimi_sepide@yahoo.com

***Corresponding Author:** Simin Ganjei,*
Department of Water Engineering, Faculty of Agriculture, University of Tabriz, Tabriz, Iran.
Email: siminganjei@yahoo.com.

Abstract

Agriculture aims for effective resource management techniques, such as calculating irrigation needs, to maximize agricultural productivity. Reference evapotranspiration (ET_0), an important component of the hydrological cycle, has important role in agricultural operations, particularly irrigation and drainage plans. This research aims to evaluate the accuracy of the Hargreaves-Samani (HS) model in the two stages of calibration and validation and comparing with gene expression programming (GEP) in daily ET_0 modeling. In addition, interpolation techniques, such as ordinary kriging (OK) and inverse distance weighting (IDW) for the spatial distribution of ET_0 in northwest Iran were utilized. The meteorological data of 43 synoptic stations in northwestern Iran were used. FAO Penman-Monteith (FAO56 PM) model was used as benchmark of assessing the rest of the models. Models were evaluated according to five performance indices such as the root mean square error (RMSE), the scatter index (SI), the Nash-Sutcliffe coefficient (NS), the coefficient of determination (R^2) and the coefficient of residual mass (CRM). According to the obtained results, the accuracy of the HS model decreases with calibration. The GEP model has better performance than the HS model, which has high accuracy in estimating ET_0 at the Urmia station with a statistical index of R^2=0.945, RMSE=0.543 mm, SI=0.149, NS=0.944 and CRM=0.003. The maps of the spatial distribution of ET_0 were produced with the IDW interpolation method, which provided the best estimates.

Keywords: Calibration, Evapotranspiration, GEP, Hargreaves-samani, Interpolation.

Introduction

Crop water requirement called sometimes as evapotranspiration (ET) is an important parameter of the energy and water balance, especially in semi-arid and arid areas, so accurate prediction of ET is essential for research studies related to hydrology, meteorology, agriculture, and drainage system design, assessing floods

and drought periods etc (1, 2). FAO Penman-Monteith's equation is one of the most frequently utilized indirect techniques for predicting reference evapotranspiration (ET_0). Using plant coefficients, this approach calculates the water demand of the required plant after determining the water requirement of the reference plant, e.g grass (3). Solar radiation, relative humidity, wind speed, and minimum and maximum air temperature, along with some other factors are required by the FAO Penman-Monteith reference method, which are typically inaccurate or unavailable in some regions (4). The Hargreaves-Samani (HS) model is one of the empirical equations to estimate ET_0 that needs only the daily maximum temperature and minimum temperature as necessary meteorological variables (3, 5). In addition to empirical equations, substantial researches have been done recently on the complex and non-linear process of ET_0 estimation utilizing soft computing techniques.

Ogunrinde *et al*. (2022) evaluated the calibrated versions of the Hargreaves-Samani (HS) model by using the Penman-Monteith (FAO-56 PM) equation as benchmark (6). There was an overall improvement in the HS model after calibration in the Northern Region of Nigeria (NRN). However, the model improvement was more obvious in sub-humid and humid regions. Zhu *et al*. (2019) used the data from 838 Chinese stations to compare the original HS model with its calibrated versions and confirmed the better performance of the calibrated HS model in most of the climate zones (7). Feng *et al*. (2017) utilized data from 19 meteorological stations at China to evaluate the calibrated the HG model and found that the both original and calibrated HS models overestimated ET_0 on different time scales (8). However, the calibrated HS model generated average values that were closer to FAO56 PM ET_0, which could suggest the calibrated HS model's strong performance. A lot of research has been conducted worldwide to validate and calibrate the HS model under a variety of climatic situations (9-12). However, as such calibrations are generally location-specific, they cannot be applied to other locations with very different climates.

Mehdizadeh *et al*. (2017) investigated gene expression programming (GEP), multivariate regression (MARS) and support vector machine (SVM), along with some other equations for mean monthly ET0 estimations in Iran. Based on their report, the performances of the GEP, MARS and SVM models were better than the used equations (13). Shiri *et al*. (2015); Alqifari (2023) calibrated the HS model using the meteorological parameters of 29 meteorological stations in Iran and compared it with the GEP model with the same input variables (14, 15). Their research showed that the performance of the GEP model is better than that of HS. Shiri *et al*. (2013) compared machine learning models with empirical ET_0 estimation equations and confirmed their generalization ability (16). Gavili *et al*. (2018) compared the Makkink, Hargreaves-Samani, Hargreaves, Makkink-Hansen and Priestley-Taylor equations with the GEP, neuro-fuzzy and neural networks from five stations located in Iran. The outcome shows that when modeling daily ET_0, the later models offered better accuracy level, when compared to the first group (17). Further, Spontoni *et al*. (2023); Bayram and Çıtakoğlu, (2023); Ikram *et al*. (2022), Shiri *et al*. (2019) used soft computing models to estimate ET_0, and showed that these models are highly accurate at predicting ET_0 when compared to traditional empirical equations (18-21).

With digging into spatial modeling scenarios, Yildirim *et al*. (2023), Bahamid (2022) investigated several interpolation techniques, such as radial basis function, inverse distance weighted (IDW), co-kriging, and ordinary kriging (OK), and compared them to create the best ET_0 maps for Türkiye (22, 23). Hodam *et al*. (2017) and Prasanth (2022) examine the spatial distribution of ET_0 over India using IDW interpolation and Kriging methods (24, 25). The result of their research shows that Kriging performed better for cross-validation, but IDW performed better in station-wise validation. Raziei and Pereira (2013) used 148 weather stations from Iran during the 1991–2005 for interpolation (26). The OK method and a spherical isotropic variogram were used. Results showed identical spatial patterns of ET_0, with the lowest values in northern humid and sub-humid climates and larger values in arid and hyper-arid regions. Bostan *et al*. (2012); Genc (2022) compared five statistical methods to predict Turkey's average annual precipitation using point observations and spatially exhaustive covariate data (27, 28). The study found that universal kriging was the most accurate.

Considering the significance of accurate ET_0 calculation in the planning, designing, and administering of irrigation networks and systems, this study assessed the temperature-based Hargreaves-Samani empirical model's accuracy for spatial simulation of ET_0. A comparison was performed between HS and GEP, too. On the other hand, due to the limited number of synoptic stations, the geographical information system (GIS) was used to estimate ET_0 at unmeasured points for zoning. So geostatistical methods were compared with each other, and daily reference evapotranspiration was zoned in northwest Iran.

Materials and Methods

Study Area

Iran is a country in southwest Asia and the northern hemisphere, covering an area of more than 1,648,000 km^2. In this research, meteorological data of 43 synoptic stations in northwestern Iran, obtained from the Islamic Republic of Iran Meteorological Organization (IRIMO), was used in daily scales. These stations included the Ardabil, West Azerbaijan, East Azerbaijan, Hamedan, Kurdistan and Zanjan provinces **(Figure 1)**. The statistical data period was used for ten years (2009-2019). Minimum air temperature (T_{min}), Maximum air temperature (T_{max}), wind speed at 2 m height (u_2), solar radiation (R_s) and relative humidity (RH), are used. The general details of the station under study, along with their meteorological parameters, are compiled in **Table 1**.

The aridity index (I_A), a numerical indicator of dryness degree (29), was computed for all stations:

$$I_A = \frac{P}{ET_0} \quad (1)$$

where P is the total annual precipitation (mm) and ET_0 is the total annual ET_0 (mm). I_A<0.03 denoted the hyper-arid region, 0.03 <I_A <0.2 shows the dry region, 0.2 <I_A<0.5 shows the semi-arid region, 0.5 <I_A <0.65 belongs to the semi-humid region and 0.65 <I_A is the humid climate. Aridity index values of the stations have been listed in **Table 1**.

The Continentality index values (CI^{CU}) is obtained based on the following equation:

$$CI^{CU} = \frac{M_i - m_i}{1 + (\frac{\theta}{3})} \quad (2)$$

where M_i and m_i are the maximum and minimum average monthly temperature (^{o}C), respectively, while θ shows the latitude of each location (degrees).

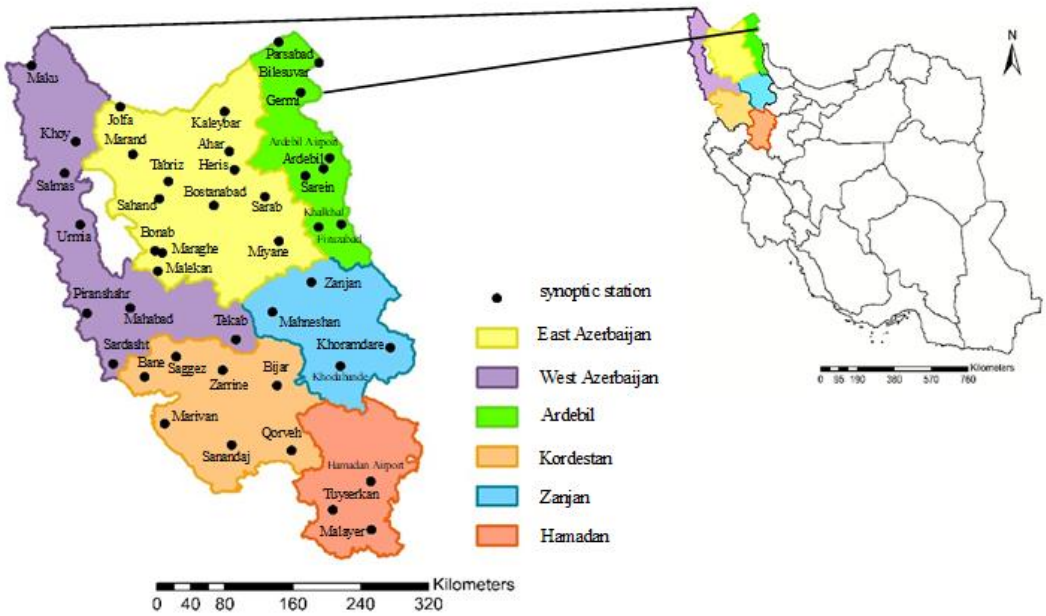

Figure 1. Geographical location of the synoptic stations in northwest Iran.

Table 1. Summary of the studied stations and data

Province	Station	Station code	Latitude (°N)	Longitude (°E)	Height (m)	T_{mean} (°C)	ΔT (°C)	$\overline{ET_0}$ (mm/day)	I_A	CI^{CU}	U_2 (m/s)	$\bar{P}$ (mm)	R_a (MJ/m².day)
Ardebil	Ardebil	1	38.22	48.33	1335.2	10.368	12.513	3.123	0.229	4.614	2.768	0.716	28.880
	Ardebil Airport	2	38.33	48.42	1314.3	9.332	14.168	3.256	0.191	4.907	3.752	0.621	28.841
	Bilesuvar	3	39.37	48.32	101.4	16.586	10.253	3.611	0.261	4.079	2.969	0.942	28.477
	Firuzabad	4	37.59	48.24	1175.7	14.183	15.654	4.057	0.174	5.181	2.563	0.706	29.098
	Germi	5	39.05	48.06	749	14.744	8.270	3.354	0.237	3.845	2.409	0.794	28.588
	Parsabad	6	39.60	47.78	72.6	15.223	11.233	3.141	0.248	4.028	1.928	0.778	28.392
	Sarein	7	38.15	48.08	1658.3	10.913	10.811	3.128	0.330	4.491	2.341	1.033	28.905
	Khalkhal	8	37.61	48.54	1797.4	9.466	12.854	3.046	0.315	4.558	1.698	0.961	29.091
West Azerbaijan	Mahabad	9	36.75	45.72	1351.8	14.111	13.064	3.794	0.250	4.603	1.975	0.950	29.382
	Maku	10	39.38	44.39	1411.2	11.548	10.498	3.117	0.294	4.332	1.683	0.916	28.471
	Piranshahr	11	36.70	45.15	1443.5	14.015	11.395	3.613	0.540	4.413	2.036	1.950	29.401
	Salmas	12	38.22	44.85	1339.3	11.920	13.043	3.720	0.191	4.353	2.376	0.711	28.881
	Sardasht	13	36.15	45.49	1556.8	14.309	8.292	3.840	0.600	3.970	2.016	2.304	29.586
	Tekab	14	36.40	47.10	1817.2	10.629	14.609	3.351	0.245	4.645	1.599	0.820	29.503
	Urmia	15	37.66	45.06	1328	12.077	13.940	3.638	0.242	4.243	2.009	0.879	29.074
	Khoy	16	38.56	45.00	1103.4	13.527	13.280	3.168	0.251	4.533	1.251	0.795	28.761
East Azerbaijan	Ahar	17	38.43	47.07	1391	11.778	11.768	3.409	0.230	4.294	2.384	0.784	28.805
	Bonab	18	37.37	46.05	1281	15.816	12.942	3.688	0.192	4.607	1.718	0.708	29.173
	Bostanabad	19	37.85	46.84	1736	11.472	13.162	3.718	0.252	4.582	3.049	0.935	29.007
	Heris	20	38.23	47.13	1950	10.576	10.022	3.325	0.319	4.133	2.388	1.061	28.875
	Jolfa	21	38.93	45.60	736.2	15.607	11.897	4.021	0.167	4.479	1.986	0.673	28.629
	Kaleybar	22	38.87	47.02	1180	13.046	8.781	3.217	0.361	3.855	2.486	1.162	28.653
	Malekan	23	37.15	46.08	1302	15.544	14.255	4.036	0.183	4.722	2.265	0.740	29.248
	Maraghe	24	37.35	46.15	1344	14.121	11.669	4.561	0.149	4.432	2.781	0.678	29.180
	Marand	25	38.42	45.77	1550	13.424	8.493	3.541	0.320	3.998	1.872	1.134	28.811
	Miyane	26	37.45	47.70	1110	14.623	13.491	3.672	0.200	4.791	1.392	0.734	29.145
	Sahand	27	37.93	46.12	1641	12.506	8.960	4.112	0.148	3.943	2.862	0.607	28.979
	Sarab	28	37.93	47.53	1682	9.416	14.566	3.410	0.186	4.691	2.232	0.635	28.979
	Tabriz	29	38.12	46.24	1361	13.542	11.773	4.311	0.171	4.304	2.685	0.739	28.913
Hamadan	Hamadan Airport	30	34.87	48.53	1740.8	12.681	16.211	3.838	0.214	5.236	1.774	0.822	30.006
	Malayer	31	34.25	48.86	1776.5	14.205	14.622	4.378	0.230	4.655	2.423	1.007	30.206
	Tuyserkan	32	34.55	48.43	1783.2	13.980	12.796	3.468	0.340	4.330	1.208	1.179	30.110
Kordestan	Bane	33	36.01	45.90	1600	14.078	10.544	4.143	0.452	4.338	2.411	1.871	29.633
	Bijar	34	35.89	47.62	1883.4	12.215	11.492	3.954	0.240	4.467	2.410	0.949	29.673
	Marivan	35	35.50	46.15	1287	13.740	16.864	3.465	0.663	5.026	1.297	2.295	29.801
	Qorveh	36	35.18	47.79	1906	13.028	11.848	3.948	0.221	4.675	2.147	0.872	29.905
	Sanandaj	37	35.25	47.01	1373.4	14.788	16.738	3.925	0.252	4.862	1.582	0.989	29.881

	Saggez	38	36.22	46.31	1522.8	12.030	16.347	3.617	0.335	5.270	1.797	1.211	29.561
	Zarrine	39	36.07	46.92	2142.6	9.202	13.268	3.646	0.268	4.592	2.846	0.977	29.613
Zanjan	Mahneshan	40	36.74	47.68	1284.5	15.846	13.528	4.269	0.164	4.922	2.391	0.702	29.387
	Khodabande	41	36.14	48.59	1887	11.775	11.136	3.934	0.288	4.460	2.667	1.134	29.587
	Khoramdare	42	36.20	49.21	1575	12.978	12.861	3.798	0.222	4.409	2.180	0.844	29.570
	Zanjan	43	36.66	48.52	1659.4	12.435	14.502	3.463	0.233	4.803	1.566	0.807	29.414

Fao-56. Penman-Monteith Model

The following Eq. 3 describes the FAO-56 Penman-Monteith (FPM) technique of daily ET_0 estimation:

$$ET_0 = \frac{0.408 \times \Delta(R_n - G) + \gamma \frac{900}{T_{mean} + 273} U_2(e_a - e_d)}{\Delta + \gamma(1 + 0.34U_2)} \quad (3)$$

Where ET_0: reference evapotranspiration (mm/day), Δ: slope of the saturation vapor pressure function (kPa/°C), γ: psychrometric constant (kPa/°C), R_n: net solar radiation (MJ/m^{2}day), G: Soil heat flux density (MJ/m^{2}day), T_{mean}: mean air temperature (°C), U_2: is the mean wind speed at 2 meters above the soil surface (m/s), e_a: saturation vapor pressure (kPa), e_d: actual vapor pressure (kPa). This technique is a standard method to evaluate the accuracy of the other models as advised by the literature.

HS Model

When Hargreaves and Samani (1985) first introduced the HS model (Eq. 4). All that is needed to determine ET_0 by HS model is air temperature data (30).

$$ET_{HS}=0.0023(T_{mean}+17.8)\times(T_{max}-T_{min})^{0.5}\times R_a \quad (4)$$

where T_{max} and T_{min} are the maximum and minimum air temperatures (°C), respectively.

Eq. 5 was used to determine the extraterrestrial radiation data (Ra) based on day of year and station latitude.

$$R_a = \frac{24(60)}{\pi} G_{sc} d_r [\omega_s \sin(\varphi) \sin(\delta) + \cos(\varphi) \cos(\delta) \sin(\omega_s)] \quad (5)$$

Here, Ra is the extraterrestrial radiation (MJ/m^2.day), G_{SC} is the solar constant (0.0820 MJ/m^2.min), ω_S is the sunset hour angle (rad), d_r is the inverse relative Earth-Sun distance, δ is the solar declination (rad) and φ is the latitude (rad). To convert the unit of extraterrestrial radiation into the equivalent unit of ET_0 (mm/day), its values should be multiplied by 0.408.

Regression technique (Eq. 6) was utilized to generate the adjusted (calibrated) HS model, which is a commonly known and used method (31).

$$ET_0^{FAO56\text{-}PM}=\alpha ET_0^{HS}+\beta \quad (6)$$

where α and β are regression coefficients, ET_0^{FPM} is estimated by FAO56-PM and ET_0^{HS} is estimated by the Hargreaves-Samani model. For this purpose, 70% of the patterns were selected for calibration of the HS model and 30% of the patterns were used for validation (testing).

Gene Expression Programming (GEP)

In GEP, chromosomes (individuals) are linear entities with fixed lengths that express the genetic information that has been encoded. Afterward, the genetic data is eventually transformed into non-linear structures (expression trees or computer programs) of different lengths and sizes. One or more genes, each of which codes for a smaller subprogram known as a genotype, can be found on chromosomes. Then, through a random generation process, every chromosome in the original population is expressed (phenotyped). The fitness of every single chromosome is assessed using a series of fitness function equations (32). After being modified and reevaluated by the genetic operators through recombination, inversion, transposition, and mutation, the chromosomes with superior solutions are then chosen based on their fitness values. To determine the right resolve (chromosomes) and attain the necessary accuracy, this process is repeated (33).

Selecting the fitness function, a set of terminals and functions, the chromosomal structure, the linking function, and the genetic operators are the steps involved in modeling ET_0 using the GEP model.
Meteorological parameters such as extraterrestrial radiation data (Ra), Tmax and Tmin for ten years were selected as the inputs for this model, while ET_0 was the target parameter. The same training and testing partitions of HS calibration was used here for GEP.

Interpolation Methods
The two primary types of interpolation approaches are geostatistical (stochastic) and deterministic methods. In the first group methods, the surface is generated from sample points based on the degree of similarity using mathematical functions to generate surfaces from. But stochastic methods, like Kriging, evaluate uncertainty using statistical and mathematical characteristics (24).

Inverse Distance Weighting (IDW)
As a simple and most popular interpolation techniques used in hydrology, IDW (34) is a deterministic interpolation method that uses weights on the data points that decrease in significance as they get farther away from the data point. IDW method's mathematical model can be expressed as follows:

$$X^* = \frac{\sum_{i=1}^{n} \frac{x_i}{D_i^p}}{\sum_{i=1}^{n} \frac{1}{D_i^p}} \quad (7)$$

X* is the calculated value, n indicates the total number of values in the sample data, xi is the ith data value, D_i shows the distance of separation between the sample data value and the interpolated value and P displays the power of weighing.

Ordinary Kriging
Kriging modifies a mathematical function to include all points (or a certain number of points) inside a given radius. For every pre-defined point, the interpolated value can be obtained via this function. A hypothesis by this method dictates that the variations in the observed variable surface can be explained by a spatial correlation that is reflected in the direction and distance between the sample points. In this study, Ordinary Kriging was utilized, which is considered as one of the most popular techniques for spatial prediction (35).

$$Y^*(x) = \sum_{i=1}^{n} \lambda_i Y(x_i) \quad (8)$$

where Y*(x) shows the unsampled location, x_i is the representative of the sample location and λ is the assigned weight to each observed sample.

Study Flowchart
HS model was used and calibrated using data from 43 stations. Then, the GEP model with the same inputs of HS i.e., temperature and extraterrestrial radiation were implemented and tested at the same locations. FAO56-PM model was used to assess the performance of these models. Then, some interpolations methods were utilized to spatial interpolation of the ET_0 values. **Figure 2** displays the ET_0 prediction workflow adopted in the present study.

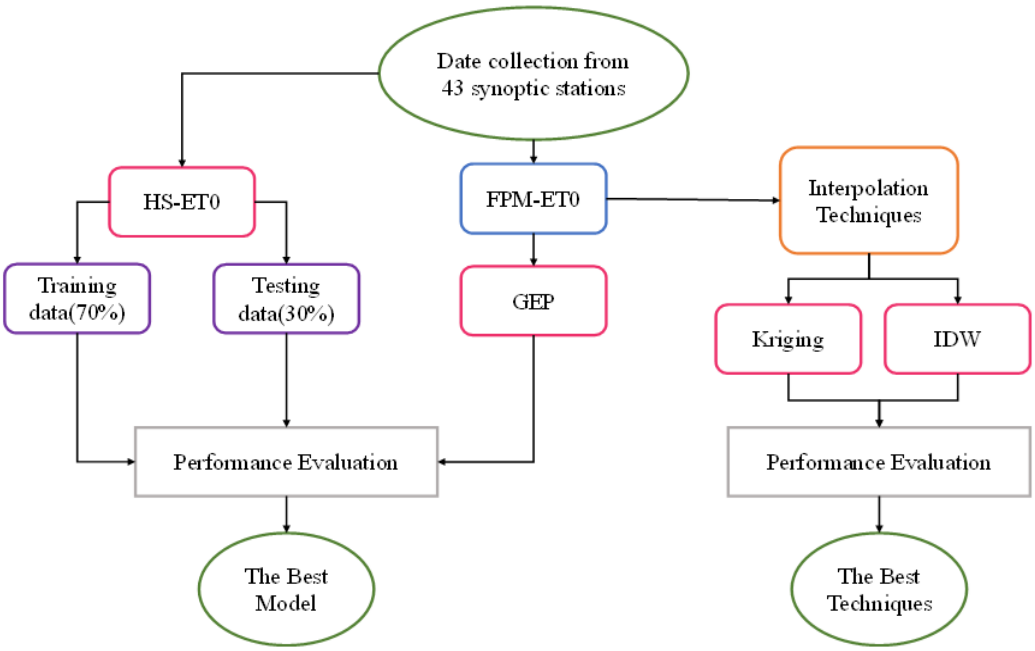

Figure 2. ET0 prediction workflow

Evaluation Criteria

The accuracy of the model was evaluated using several common statistical criteria, such as the root mean square error (RMSE), the scatter index (SI), the Nash Sutcliffe coefficient (NS), the coefficient of determination (R^2) and the coefficient of residual mass (CRM):

$$RMSE = \sqrt{\frac{1}{N}\sum_{i=1}^{N}(ET_m - ET_o)^2} \quad (9)$$

$$SI = \frac{RMSE}{\overline{ET_0}} = \frac{\sqrt{\frac{1}{N}\sum_{i=1}^{N}(ET_m - ET_o)^2}}{\overline{ET_o}} \quad (10)$$

$$NS = 1 - \frac{\sum_{i=1}^{N}(ET_m - ET_o)^2}{\sum_{i=1}^{N}(ET_o - \overline{ET_o})^2} \quad (11)$$

$$R^2 = [\frac{\sum_{i=1}^{N}(ET_m - \overline{ET_m})(ET_o - \overline{ET_o})}{\sqrt{\sum_{i=1}^{N}(ET_m - \overline{ET_m})^2 \sum_{i=1}^{N}(ET_o - \overline{ET_o})^2}}]^2 \quad (12)$$

$$CRM = \frac{(\sum_{i=1}^{N} ET_0 - \sum_{i=1}^{N} ET_m)}{\sum_{i=1}^{N} ET_0} \quad (13)$$

where ET_m and ET_0 define the values obtained by using the HS/GEP models and by the FAO56-PM ET_0 equation respectively; N is the number of data sets; and $\overline{ET_0}$ and $\overline{ET_m}$ represent the mean ET values estimated by FAO56-PM and HS/GEP, respectively.

Results and Discussion

Performance of HS Method

Meteorological data from 2009 to 2016 were considered as the training stage, while the rest of the available data (2017-2019) was used as the testing data. The statistical index results for the Hargreaves Samani equation's test and training stages and regression coefficient are shown in **Tables 2 and 3**. According to the obtained results, in the calibration stage (training) at Urmia station with values of R^2=0.950, RMSE=0.535

mm, SI=0.149, NS=0.943 and CRM=0.051 is the best and at Sahand station with values of R^2=0.894, RMSE =1.833 mm, SI=0.444, NS=0.603 and CRM=0.318 showed the weakest performance. In the validation stage (testing), this method has the best performance at Urmia station with values of R^2=0.958, RMSE=0.676 mm, SI=0.181, NS=0.920 and CRM=0.110 and at Sahand station with values of R^2=0.905, RMSE=2.705 mm, SI= 0.666, NS=0.147 and CRM=0.492 have the weakest performance. As a result, the original non-calibrated Hargreaves-Samani equation performed well in Iran's northwest. According to Xu *et al*. (2013); Haidar (2022), which concluded that Hargreaves-Samani calibration reduces its accuracy, it is in the same direction (36, 37).

Table 2. Statistics index of the Hargreaves-Samani (2009-2016)

Station	Station Code	Train (Calibration)					Regression coefficient	
		R^2	RMSE	SI	NS	CRM	a	b
Ardebil	**1**	0.8	0.889	0.287	0.786	0.046	0.881	0.224
Ardebil Airport	**2**	0.852	0.835	0.26	0.836	0.081	0.843	0.244
Bilesuvar	**3**	0.876	1.09	0.296	0.845	0.103	0.773	0.456
Firuzabad	**4**	0.863	1.045	0.256	0.855	0.055	0.834	0.455
Germi	**5**	0.836	1.399	0.41	0.716	0.197	0.622	0.617
Parsabad	**6**	0.895	0.738	0.24	0.888	-0.055	0.924	0.404
Sarein	**7**	0.817	0.953	0.302	0.793	0.101	0.785	0.359
Khalkhal	**8**	0.805	0.917	0.299	0.796	0.06	0.831	0.334
Mahabad	**9**	0.822	1.037	0.273	0.807	0.062	0.888	0.192
Maku	**10**	0.897	0.743	0.239	0.879	0.084	0.846	0.218
Piranshahr	**11**	0.821	1.013	0.278	0.798	0.09	0.85	0.219
Salmas	**12**	0.938	0.816	0.22	0.896	0.115	0.822	0.234
Sardasht	**13**	0.885	1.489	0.38	0.669	0.264	0.662	0.29
Tekab	**14**	0.893	0.758	0.226	0.887	-0.016	0.966	0.168
Urmia	**15**	**0.95**	**0.535**	**0.149**	**0.943**	**0.051**	0.94	0.033
Khoy	**16**	0.884	0.823	0.261	0.84	-0.099	1.021	0.246
Ahar	**17**	0.857	0.843	0.25	0.818	0.107	0.926	-0.11
Bonab	**18**	0.833	1.024	0.277	0.832	-0.003	0.857	0.54
Bostanabad	**19**	0.902	0.902	0.24	0.863	0.127	0.887	-0.054
Heris	**20**	0.908	0.936	0.28	0.838	0.163	0.791	0.154
Jolfa	**21**	0.776	1.698	0.421	0.709	0.144	0.776	0.97
Kaleybar	**22**	0.881	0.992	0.301	0.792	0.184	0.78	0.116
Malekan	**23**	0.841	1.035	0.261	0.838	0.034	0.861	0.419
Maraghe	**24**	0.912	1.739	0.381	0.678	0.27	0.655	0.342
Marand	**25**	0.879	1.21	0.34	0.755	0.212	0.719	0.245
Miyane	**26**	0.855	1.001	0.276	0.854	-0.012	0.835	0.643
Sahand	**27**	0.894	1.833	0.444	0.603	0.318	0.615	0.276
Sarab	**28**	0.897	0.734	0.217	0.888	0.061	0.92	0.066
Tabriz	**29**	0.89	1.593	0.369	0.717	0.237	0.667	0.415
Hamadan Airport	**30**	0.889	0.823	0.216	0.87	-0.021	1.017	0.018
Malayer	**31**	0.885	1.007	0.227	0.823	0.133	0.926	-0.261
Tuyserkan	**32**	0.871	0.81	0.233	0.855	-0.035	0.979	0.197
Bane	**33**	0.891	1.406	0.335	0.723	0.237	0.728	0.15
Bijar	**34**	0.833	1.416	0.343	0.7	0.221	0.75	0.119
Marivan	**35**	0.891	1.062	0.31	0.743	-0.173	1.137	0.124

Qorveh	**36**	0.878	1.063	0.266	0.799	0.165	0.842	-0.029
Sanandaj	**37**	0.855	1.003	0.253	0.827	-0.049	0.991	0.232
Saggez	**38**	0.892	0.829	0.227	0.874	-0.033	1.01	0.084
Zarrine	**39**	0.912	0.895	0.247	0.863	0.139	0.842	0.068
Mahneshan	**40**	0.852	1.155	0.262	0.811	0.121	0.864	0.064
Khodabande	**41**	0.847	1.373	0.346	0.719	0.216	0.723	0.24
Khoramdare	**42**	0.882	0.904	0.237	0.852	0.104	0.855	0.153
Zanjan	**43**	0.908	0.691	0.199	0.889	-0.018	1.036	-0.061

Table 3. Statistics index of the Hargreaves-Samani (2017-2019)

Station	**Station code**	**HS**					**Test (Validation)**				
		R^2	**RMSE**	**SI**	**NS**	**CRM**	**R^2**	**RMSE**	**SI**	**NS**	**CRM**
Ardebil	**1**	0.895	0.930	0.293	0.787	0.069	0.801	0.971	0.306	0.767	0.109
Ardebil Airport	**2**	0.930	0.850	0.254	0.843	0.095	0.866	1.026	0.307	0.771	0.164
Bilesuvar	**3**	0.935	0.944	0.274	0.860	0.058	0.875	1.242	0.36	0.758	0.14
Firuzabad	**4**	0.937	1.035	0.259	0.868	0.044	0.878	1.232	0.308	0.813	0.09
Germi	**5**	0.914	1.129	0.352	0.776	0.122	0.835	1.683	0.524	0.502	0.262
Parsabad	**6**	0.946	0.744	0.226	0.894	-0.023	0.895	0.784	0.238	0.883	-0.068
Sarein	**7**	0.913	0.849	0.276	0.812	0.093	0.834	1.038	0.338	0.72	0.171
Khalkhal	**8**	0.912	0.834	0.279	0.823	-0.002	0.832	0.844	0.282	0.819	0.055
Mahabad	**9**	0.892	1.129	0.299	0.783	0.027	0.796	1.143	0.303	0.778	0.086
Maku	**10**	0.947	0.725	0.232	0.890	0.050	0.896	0.893	0.286	0.833	0.126
Piranshahr	**11**	0.897	1.028	0.290	0.793	0.046	0.805	1.108	0.313	0.76	0.128
Salmas	**12**	0.968	0.825	0.220	0.902	0.105	0.938	1.224	0.327	0.783	0.201
Sardasht	**13**	0.947	1.195	0.326	0.764	0.207	0.897	1.987	0.542	0.347	0.396
Tekab	**14**	0.953	0.747	0.223	0.903	-0.045	0.909	0.751	0.224	0.902	-0.059
Urmia	**15**	**0.979**	**0.550**	**0.147**	**0.947**	**0.062**	**0.958**	**0.676**	**0.181**	**0.92**	**0.11**
Khoy	**16**	0.942	0.855	0.267	0.846	-0.106	0.887	1.04	0.325	0.772	-0.206
Ahar	**17**	0.933	0.830	0.239	0.838	0.097	0.871	1.005	0.289	0.762	0.195
Bonab	**18**	0.920	0.987	0.269	0.844	-0.013	0.846	1.016	0.276	0.835	-0.015
Bostanabad	**19**	0.953	0.776	0.216	0.898	0.069	0.909	1.022	0.284	0.823	0.189
Heris	**20**	0.959	0.855	0.259	0.871	0.131	0.919	1.315	0.399	0.694	0.266
Jolfa	**21**	0.892	1.615	0.404	0.736	0.131	0.795	1.805	0.451	0.671	0.083
Kaleybar	**22**	0.952	0.725	0.239	0.878	0.101	0.905	1.157	0.381	0.689	0.26
Malekan	**23**	0.934	1.024	0.243	0.861	0.069	0.873	1.143	0.272	0.826	0.1
Maraghe	**24**	0.954	1.655	0.363	0.717	0.247	0.91	2.664	0.584	0.266	0.432
Marand	**25**	0.946	1.113	0.318	0.801	0.184	0.895	1.736	0.496	0.516	0.343
Miyane	**26**	0.942	0.958	0.254	0.883	0.007	0.887	1.109	0.294	0.843	0.001
Sahand	**27**	0.951	1.686	0.415	0.669	0.285	0.905	2.705	0.666	0.147	0.492
Sarab	**28**	0.948	0.770	0.222	0.889	0.067	0.9	0.863	0.249	0.861	0.123
Tabriz	**29**	0.948	1.575	0.367	0.730	0.232	0.898	2.423	0.564	0.362	0.391
Hamadan Airport	**30**	0.963	0.677	0.173	0.922	0.010	0.926	0.687	0.176	0.92	-0.011

Malayer	**31**	0.950	0.824	0.194	0.874	0.082	0.903	1.152	0.272	0.753	0.211
Tuyserkan	**32**	0.948	0.717	0.208	0.891	-0.034	0.899	0.738	0.214	0.885	-0.069
Bane	**33**	0.957	1.865	0.463	0.493	0.171	0.916	1.865	0.463	0.493	0.36
Bijar	**34**	0.948	0.776	0.218	0.881	0.080	0.898	1.31	0.369	0.662	0.277
Marivan	**35**	0.978	0.834	0.234	0.852	-0.144	0.957	1.529	0.429	0.502	-0.336
Qorveh	**36**	0.948	0.887	0.232	0.857	0.123	0.899	1.34	0.35	0.674	0.269
Sanandaj	**37**	0.934	1.029	0.269	0.802	-0.091	0.873	1.099	0.287	0.773	-0.142
Saggez	**38**	0.958	0.802	0.226	0.877	-0.074	0.917	0.862	0.243	0.858	-0.108
Zarrine	**39**	0.965	0.909	0.247	0.872	0.151	0.931	1.336	0.362	0.723	0.267
Mahneshan	**40**	0.932	0.932	0.237	0.862	0.038	0.868	1.108	0.282	0.805	0.152
Khodabande	**41**	0.936	1.222	0.317	0.780	0.188	0.877	1.882	0.488	0.479	0.35
Khoramdare	**42**	0.938	0.884	0.237	0.864	0.079	0.879	1.11	0.297	0.785	0.171
Zanjan	**43**	0.971	0.642	0.186	0.908	-0.060	0.943	0.715	0.207	0.886	-0.08

Performance of GEP

The GEP model predicted the amount of ET_0 with Ra, Tmax and Tmin inputs. The statistical results for the GEP model are shown in **Table 4**. According to the obtained results, GEP in northwestern Iran at Urmia station with values of R^2=0.945, RMSE=0.543 mm, SI=0.149, NS=0.944 and CRM=0.003 has the best performance and at Garmi station with values of R^2=0.856, RMSE=0.972 mm, SI=0.290, NS=0.855 and CRM=0.015 it has the weakest performance in reference evapotranspiration estimation. As a result, this model estimates ET_0 with good accuracy, which is in agreement with Mattar (2018); Efremov (2023) (38, 39).

Table 4. Statistics indices of the GEP model

Station	Station code	R^2	RMSE	SI	NS	CRM
Ardebil	**1**	0.812	0.85	0.272	0.81	-0.008
Ardebil Airport	**2**	0.856	0.793	0.244	0.856	0.003
Bilesuvar	**3**	0.904	0.837	0.232	0.904	0.004
Firuzabad	**4**	0.912	0.826	0.203	0.912	0.001
Germi	**5**	0.856	0.972	0.29	0.855	0.015
Parsabad	**6**	0.9	0.706	0.225	0.9	-0.006
Sarein	**7**	0.825	0.861	0.275	0.824	0.011
Khalkhal	**8**	0.923	0.56	0.184	0.923	0
Mahabad	**9**	0.861	0.886	0.233	0.861	0
Maku	**10**	0.882	0.74	0.237	0.882	-0.01
Piranshahr	**11**	0.843	0.895	0.248	0.843	0.002
Salmas	**12**	0.924	0.715	0.192	0.922	0.002
Sardasht	**13**	0.903	0.795	0.207	0.903	0
Tekab	**14**	0.913	0.677	0.202	0.913	0
Urmia	**15**	**0.945**	**0.543**	**0.149**	**0.944**	**0.003**
Khoy	**16**	0.869	0.758	0.239	0.869	-0.004
Ahar	**17**	0.87	0.723	0.212	0.87	-0.003
Bonab	**18**	0.896	0.808	0.219	0.896	0.001
Bostanabad	**19**	0.905	0.75	0.202	0.905	-0.007
Heris	**20**	0.916	0.687	0.207	0.914	-0.002
Jolfa	**21**	0.92	0.89	0.221	0.92	-0.005

Kaleybar	**22**	0.868	0.781	0.243	0.868	0.001
Malekan	**23**	0.88	0.912	0.226	0.879	-0.006
Maraghe	**24**	0.912	0.911	0.2	0.912	0.003
Marand	**25**	0.89	0.821	0.232	0.889	-0.01
Miyane	**26**	0.869	0.973	0.265	0.868	-0.004
Sahand	**27**	0.895	0.947	0.23	0.894	-0.004
Sarab	**28**	0.917	0.643	0.189	0.917	0.003
Tabriz	**29**	0.91	0.924	0.214	0.91	0.001
Hamadan Airport	**30**	0.906	0.718	0.187	0.905	0.013
Malayer	**31**	0.908	0.717	0.164	0.908	-0.002
Tuyserkan	**32**	0.9	0.678	0.196	0.9	0.012
Bane	**33**	0.918	0.763	0.184	0.918	-0.001
Bijar	**34**	0.849	0.972	0.246	0.849	0.005
Marivan	**35**	0.924	0.582	0.168	0.924	-0.003
Qorveh	**36**	0.921	0.666	0.169	0.921	0.002
Sanandaj	**37**	0.866	0.876	0.223	0.865	0
Saggez	**38**	0.915	0.675	0.187	0.915	-0.001
Zarrine	**39**	0.929	0.659	0.181	0.928	0.003
Mahneshan	**40**	0.869	0.951	0.223	0.869	-0.005
Khodabande	**41**	0.89	0.864	0.22	0.889	0.007
Khoramdare	**42**	0.902	0.739	0.195	0.902	0.001
Zanjan	**43**	0.927	0.564	0.163	0.927	0.001

Comparison of HS Equations and GEP Model

By comparing the statistical index of the original HS equation and its calibrated version with the GEP, the best method for estimating daily reference evapotranspiration in northwest Iran was determined. **Figure 3** indicates that the empirical model (Hargreaves-Samani) performs worse than the GEP. The predicted ET_0 values of two models are contrasted with the average of annual FAO Penman-Monteith ET_0 values in **Figure 4**. As can be noticed, GEP has a high degree of accuracy for estimating ET_0. Shiri *et al*. (2012); Bramhe (2022); Asfahani (2022) reported similar results, so the GEP model outperformed the empirical model (40-42).

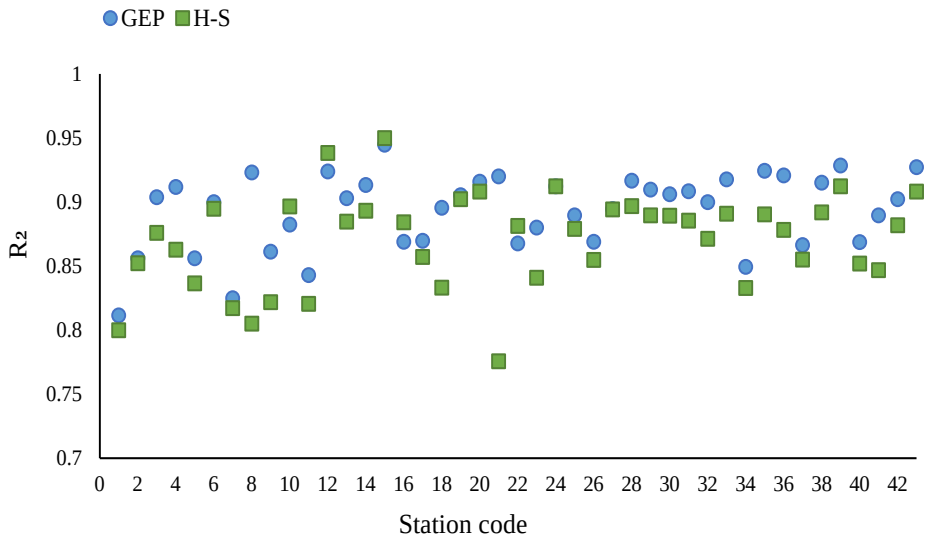

a)

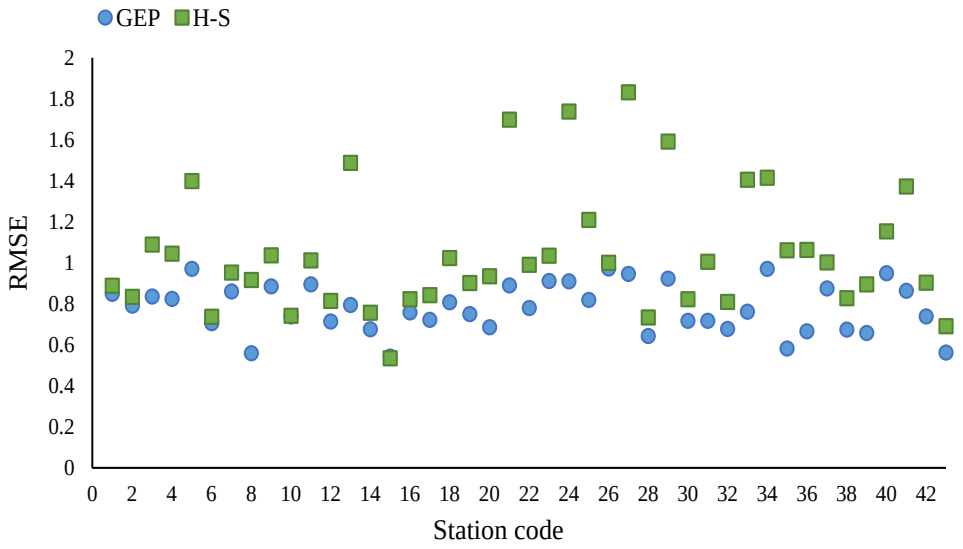
GEP
H-S
RMSE
Station code

b)

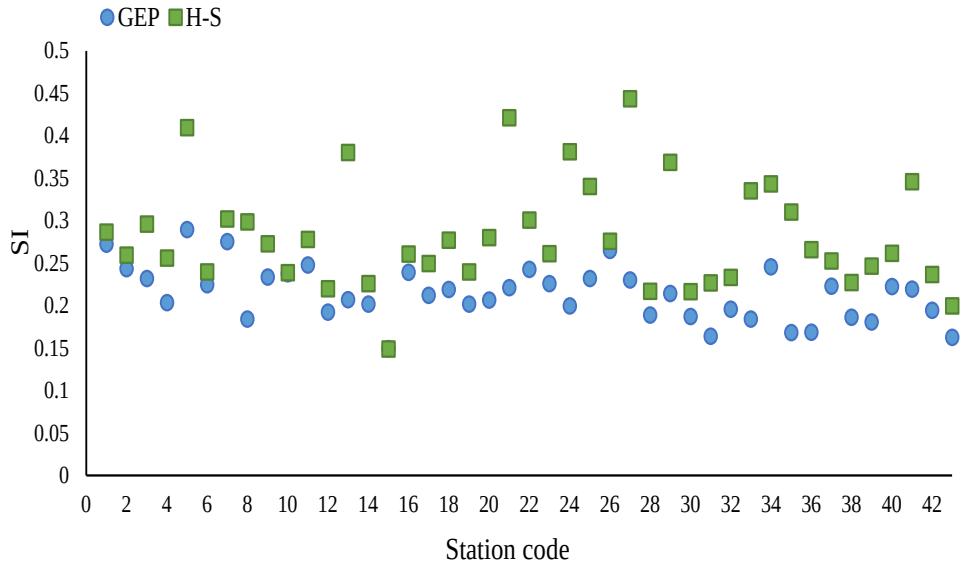
GEP
H-S
SI
Station code

c)

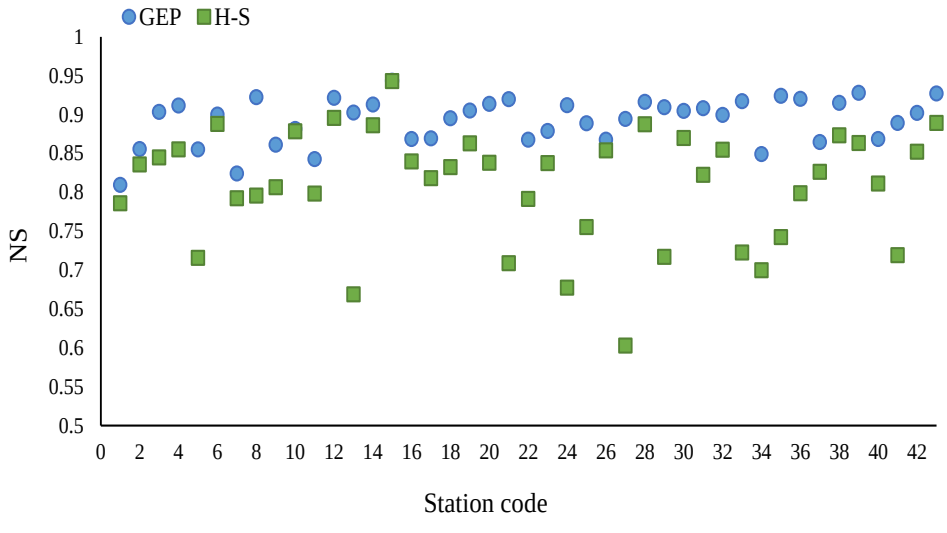
GEP
H-S
NS
Station code

d)

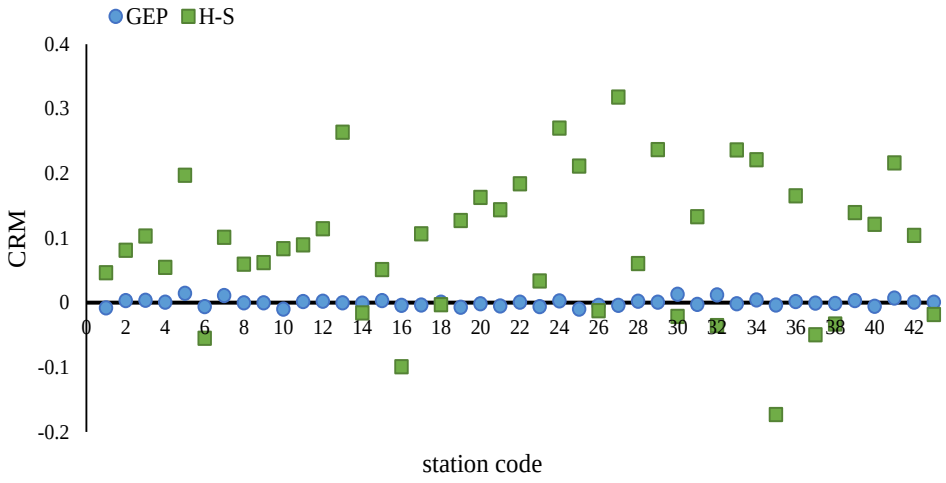

e)

Figure 3. Comparison of HS and GEP models' accuracy

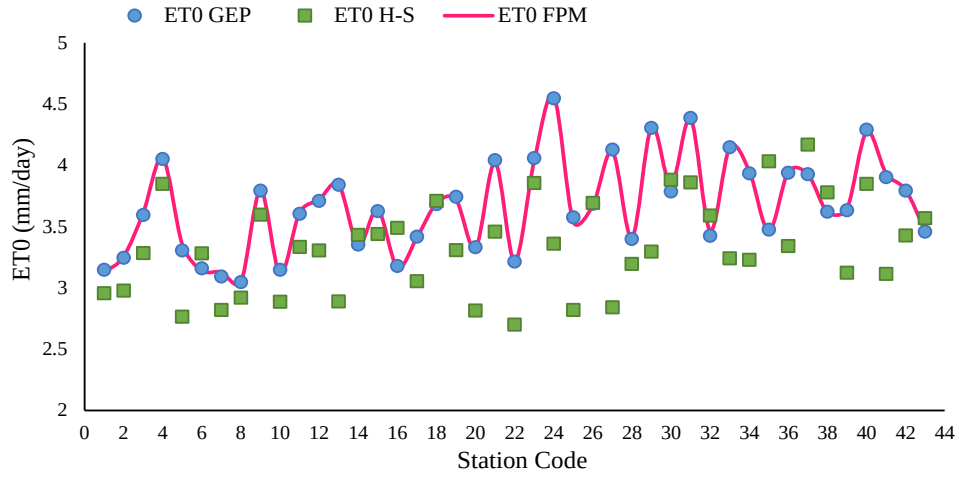

Figure 4. ET0 values of models.

Interpolation Methods

Due to the limited and expensive synoptic stations, geostatistical methods should be used to estimate ET_0 at unmeasured points for zoning. Two geostatistical methods, Kriging and IDW, were used for ET_0 zoning here. The statistical index values for two methods are displayed in **Table 5**. The findings indicate the excellent accuracy and low error of the IDW method for ET_0 zoning, which is consistent with Da Silva *et al*. (2019) and Saad *et al*. (2023) research results. **Figure 5** shows the zoning map for these two methods (43, 44). The ET_0 in northwestern Iran is in the range of (4.414–3.128) mm/day. In the stations around Lake Urmia and the southern parts of northwestern Iran, the ET_0 amount has increased, which is due to climatic conditions such as low rainfall and vegetation.

Table 5. Performance Statistics index obtained from Kiriging and IDW.

Province	Kriging					IDW				
	R^2	RMSE	SI	NS	CRM	R^2	RMSE	SI	NS	CRM
Ardebil	0.401	0.368	0.11	-0.331	-0.005	0.052	0.372	0.111	-0.359	-0.042
West Azerbaijan	0.364	0.277	0.079	-0.11	-0.05	0.208	0.32	0.091	-0.483	-0.061
East Azerbaijan	0.36	0.325	0.086	0.316	0.018	0.137	0.375	0.099	0.088	0.023
Hamadan	0.994	0.544	0.14	-1.116	0.003	0.999	0.446	0.114	-0.42	0.016
Kordestan	0.277	0.259	0.068	-0.354	0.008	0.773	0.255	0.067	-0.314	0.008
Zanjan	0.109	0.342	0.088	-0.396	0.014	0.228	0.341	0.088	-0.387	0.041

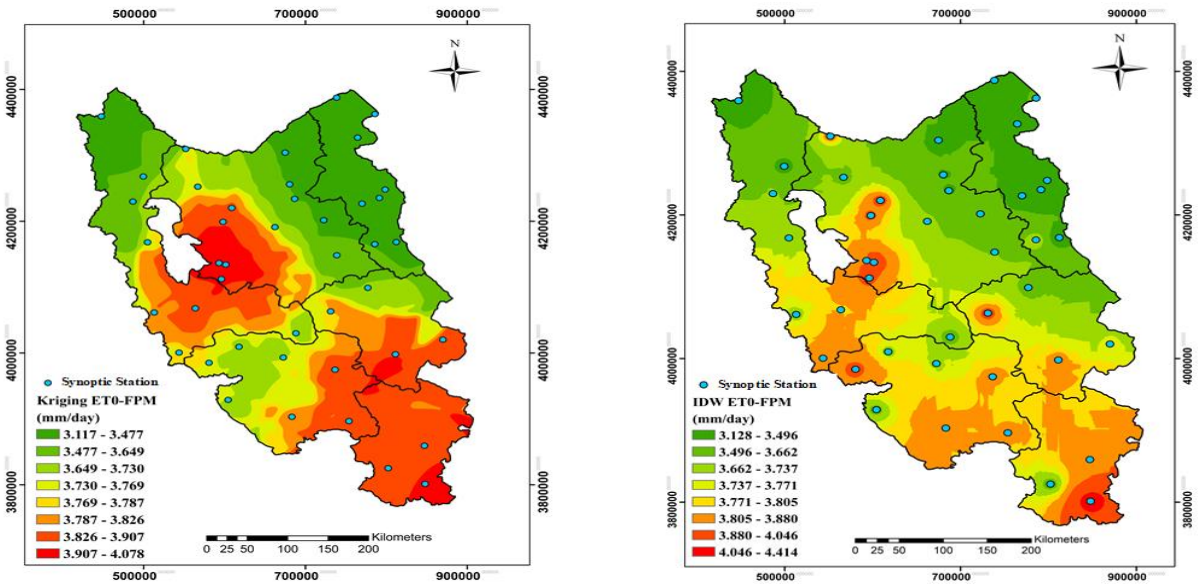

a) b)

Figure 5. Reference evapotranspiration interpolation map

Conclusion

Evapotranspiration estimation is important in these regions due to several factors, including limited renewable water resources, growing populations, incorrect water usage patterns, poor irrigation systems, and an imbalance between supply and demand for water. In this study, we the Hargreaves Samani (HS) and GEP models were used to simulate ET_0 using data from ten years period at 43 stations in northwest Iran. In these regions, ET_0 was interpolated and geostatistical techniques were used for spatial zoning. When the GEP model and Hargreaves Samani's model are compared using the same input parameters, the GEP model performs better than the empirical model. The IDW approach has a high level of accuracy in interpolating evapotranspiration, according to the evaluation results of the IDW and Kriging approaches. According to the map created around Lake Urmia and the southern parts of the studied area, the rate of ET_0 increases.

Acknowledgments: We acknowledge that the meteorological dataset utilized in this investigation was provided by the Islamic Republic of Iran Meteorological Organization (IRIMO).

Conflict of interest: None

Financial support: None

Ethics statement: None

References

1. Rivas R, Caselles V. A simplified equation to estimate spatial reference evaporation from remote sensing-based surface temperature and local meteorological data. Remote Sens Environ. 2004;93(1-2):68-76.
2. Güler M. A comparison of different interpolation methods using the geographical information system for the production of reference evapotranspiration maps in Turkey. J Meteorol Soc Japan. Ser. II. 2014;92(3):227-40.
3. Allen RG, Pereira LS, Raes D, Smith M. Crop evapotranspiration-Guidelines for computing crop water requirements-FAO Irrigation and drainage paper 56. Fao, Rome. 1998;300(9):D05109.
4. Almorox J, Quej VH, Martí P. Global performance ranking of temperature-based approaches for evapotranspiration estimation considering Köppen climate classes. J Hydrol. 2015;528:514-22.
5. Boujguenna I, Ghlalou FE, Fakhri A, Soummani A, Rais H. Anatomopathological and Epidemiological Profile of Granulosa Tumors of the Ovary: About 9 Cases. Clin Cancer Investig J. 2023;12(2):24-6. doi:10.51847/YmkLzP0SEK

6. Ogunrinde AT, Emmanuel I, Enaboifo MA, Ajayi TA, Pham QB. Spatio-temporal calibration of Hargreaves–Samani model in the Northern Region of Nigeria. Theor Appl Climatol. 2022;147(3-4):1213-28.
7. Zhu X, Luo T, Luo Y, Yang Y, Guo L, Luo H, et al. Calibration and validation of the Hargreaves-Samani model for reference evapotranspiration estimation in China. Irrig Drain. 2019;68(4):822-36.
8. Feng Y, Jia Y, Cui N, Zhao L, Li C, Gong D. Calibration of Hargreaves model for reference evapotranspiration estimation in Sichuan basin of southwest China. Agric Water Manag. 2017;181:1-9.
9. Berti A, Tardivo G, Chiaudani A, Rech F, Borin M. Assessing reference evapotranspiration by the Hargreaves method in north-eastern Italy. Agric Water Manag. 2014;140(C):20-5.
10. Cobaner M, Citakoğlu H, Haktanir T, Kisi O. Modifying Hargreaves–Samani equation with meteorological variables for estimation of reference evapotranspiration in Turkey. Hydrol Res. 2017;48(2):480-97.
11. Bautista F, Bautista D, Delgado-Carranza C. Calibration of the equations of Hargreaves and Thornthwaite to estimate the potential evapotranspiration in semi-arid and subhumid tropical climates for regional applications. Atmósfera. 2009;22(4):331-48.
12. Al Issa S, Alwaily MM, Al Hadi EM, Businnah AA, Alkadi MA, Alshehri AI. Updated Evidence in Management of Cleft Lip and Palate: Simple Review Article. Arch Pharm Pract. 2023;14(1):6-10. doi:10.51847/YeQrhkns56
13. Mehdizadeh S, Behmanesh J, Khalili K. Using MARS, SVM, GEP and empirical equations for estimation of monthly mean reference evapotranspiration. Comput Electron Agric. 2017;139(3):103-14.
14. Shiri J, Sadraddini AA, Nazemi AH, Marti P, Fard AF, Kisi O, et al. Independent testing for assessing the calibration of the Hargreaves–Samani equation: New heuristic alternatives for Iran. Comput Electron Agric. 2015;117(C):70-80.
15. Alqifari S. Warfarin Therapy Improved Migraine Headaches with Aura: A Case Report. Arch Pharm Pract. 2023;14(1):66-8. doi:10.51847/lXDZ0BFUJ7
16. Shiri J, Sadraddini AA, Nazemi AH, Kisi O, Marti P, Fard AF, et al. Evaluation of different data management scenarios for estimating daily reference evapotranspiration. Hydrol Res. 2013;44(6):1058-70.
17. Gavili S, Sanikhani H, Kisi O, Mahmoudi MH. Evaluation of several soft computing methods in monthly evapotranspiration modelling. Meteorol Appl. 2018;25(1):128-38.
18. Spontoni TA, Ventura TM, Palácios RS, Curado LF, Fernandes WA, Capistrano VB, et al. Evaluation and modelling of reference evapotranspiration using different machine learning techniques for a brazilian tropical savanna. Agronomy. 2023;13(8):2056.
19. Bayram S, Çıtakoğlu H. Modeling monthly reference evapotranspiration process in Turkey: application of machine learning methods. Environ Monit Assess. 2022;195(1):67.
20. Ikram RM, Mostafa RR, Chen Z, Islam AR, Kisi O, Kuriqi A, et al. Advanced hybrid metaheuristic machine learning models application for reference crop evapotranspiration prediction. Agronomy. 2022;13(1):98.
21. Shiri J, Nazemi AH, Sadraddini AA, Marti P, Fakheri Fard A, Kisi O, et al. Alternative heuristics equations to the Priestley–Taylor approach: assessing reference evapotranspiration estimation. Theor Appl Climatol. 2019;138:831-48.
22. Yildirim D, Küçüktopcu E, Cemek B, Simsek H. Comparison of machine learning techniques and spatial distribution of daily reference evapotranspiration in Türkiye. Appl Water Sci. 2023;13(4):107.
23. Bahamid AA, AlHudaithi FS, Aldawsari AN, Eyyd AK, Alsadhan NY, Alshahrani FA. Success of orthodontic space closure vs. Implant in the management of missing first molar: systematic. Ann Dent Spec. 2022;10(4):10.
24. Hodam S, Sarkar S, Marak AG, Bandyopadhyay A, Bhadra A. Spatial interpolation of reference evapotranspiration in India: Comparison of IDW and Kriging methods. J Inst Eng (india): Series A. 2017;98:511-24.
25. Prasanth T, Gopalakrishnan D, Kumar P. Photodynamic Therapy in Treatment of Chronic Periodontitis in Comparison with SRP: A Split-Mouth Study. Ann Dent Spec. 2022;10(3):53-8. doi:10.51847/NGXN0aVvVM
26. Raziei T, Pereira LS. Spatial variability analysis of reference evapotranspiration in Iran utilizing fine resolution gridded datasets. Agric Water Manag. 2013;126:104-18.
27. Bostan PA, Heuvelink GB, Akyurek SZ. Comparison of regression and kriging techniques for mapping the average annual precipitation of Turkey. Int J Appl Earth Obs Geoinf. 2012;19:115-26.
28. Genc A, Isler SC, Oge AE, Matur Z. Effect of Sagittal Split Osteotomy with Medpor® Porous Polyethylene Implant on Masticatory Reflex. Ann Dent Spec. 2022;10(3):12-6.

29. Middleton N, Thomas D. World Atlas of Desertification. Vol. No. Ed. 1997;2.
30. Hargreaves GH, Samani ZA. Reference crop evapotranspiration from temperature. Appl Eng Agric. 1985;1(2):96-9.
31. Shiri J, Nazemi AH, Sadraddini AA, Landeras G, Kisi O, Fard AF, et al. Comparison of heuristic and empirical approaches for estimating reference evapotranspiration from limited inputs in Iran. Comput Electron Agric. 2014;108:230-41.
32. Ferreira C. Gene expression programming: mathematical modeling by an artificial intelligence. Springer; 2006.
33. Ferreira C. Gene expression programming: a new adaptive algorithm for solving problems. arXiv preprint cs/0102027. 2001.
34. De Mesnard L. Pollution models and inverse distance weighting: Some critical remarks. Comput Geosci. 2013;52:459-69.
35. Li J, Heap AD, Potter A, Daniell JJ. Application of machine learning methods to spatial interpolation of environmental variables. Environ Model Softw. 2011;26(12):1647-59.
36. Xu J, Peng S, Ding J, Wei Q, Yu Y. Evaluation and calibration of simple methods for daily reference evapotranspiration estimation in humid East China. Arch Agron Soil Sci. 2013;59(6):845-58.
37. Haidar FT. Accounting students' perceptions on a role of distance education in their soft skills development. J Organ Behav Res. 2022;7(2):188-202. doi:10.51847/8dK1WcPfHd
38. Mattar MA. Using gene expression programming in monthly reference evapotranspiration modeling: a case study in Egypt. Agric Water Manag. 2018;198:28-38.
39. Efremov A. Eliminating Psychosomatic Pain and Negative Emotions with Dehypnosis. J Organ Behav Res. 2023;8(1):1-1. doi:10.51847/RNRhuQMtqY
40. Shiri J, Kişi Ö, Landeras G, López JJ, Nazemi AH, Stuyt LC. Daily reference evapotranspiration modeling by using genetic programming approach in the Basque Country (Northern Spain). J Hydrol. 2012;414:302-16.
41. Bramhe S, Rao S, Dhawan S. Nodular Lymphocyte Predominant Hodgkin Lymphoma: A Rare Subtype with Distinct Clinicopathological Features. Clin Cancer Investig J. 2022;11(5):23-8. doi:10.51847/XIVRdLEECT
42. Asfahani A. The Effect of Organizational Citizenship Behavior on Counterproductive Work Behavior: A Moderated Mediation Model. J Organ Behav Res. 2022;7(2):143-60. doi:10.51847/sRtILGuTSd
43. da Silva Júnior JC, Medeiros V, Garrozi C, Montenegro A, Gonçalves GE. Random forest techniques for spatial interpolation of evapotranspiration data from Brazilian's Northeast. Comput Electron Agric. 2019;166:105017.
44. Saad E, Kamaleldin M, Zaghloul A, Habib E, Mashhour K. Hypofractionated Accelerated Radiotherapy with Concurrent Chemotherapy Versus Conventional Fractionation for LAHNSCC Using IMRT/VMAT: A Pilot Study. Clin Cancer Investig J. 2023;12(2):44-50. doi:10.51847/VpFPXwghHC